Monopole resonance strengths in ^{58}Ni and ^{208}Pb

D. H. Youngblood
Cyclotron Institute, Texas A&M University, College Station, Texas 77843
(Received 23 August 1996)

Giant monopole resonance strengths were obtained from small angle inelastic alpha scattering on ^{58}Ni and ^{208}Pb using deformed potential and folding models. Folding model analyses increase the sum rule strength in both nuclei, with 160% of the $E0$ sum rule required to fit the 13.7-MeV state in Pb. Significant contributions from other multipolarities could be excluded. The $E0$ strength identified in ^{58}Ni is shown to be about 42% of that identified in ^{208}Pb. [S0556-2813(97)01402-7]

PACS number(s): 24.30.Cz, 25.55.Ci, 27.40.+z, 27.80.+w

The giant monopole resonance is of particular interest because its energy is directly related to nuclear compressibility. However, for most nuclei with $A<90$, considerably less than half of the giant monopole resonance (GMR) strength has been located in the giant resonance peaks [1]. Recently, using the new beam analysis system and MDM spectrometer at Texas A&M, extremely good peak-to-continuum ratios were obtained for giant resonances excited at small angles in 240 MeV inelastic alpha scattering. With this we were able to show [2] that more than half of the GMR strength in ^{58}Ni must lie above $E_x=25$ MeV, in sharp contrast to theoretical expectations. This could have serious implications for the compressibility of nuclear matter, which is related to the centroid of the GMR strength.

Distorted-wave Born approximation (DWBA) calculations on which the ^{58}Ni conclusions [2] were based used the deformed potential model; however, Beene *et al.* [3] have shown that a consistent agreement between electromagnetic transition strengths and those measured with light- and heavy-ion inelastic scattering for low-lying 2^+ and 3^- states can only be obtained using the folding model. However, Beene *et al.* did not discuss excitation of the monopole resonance with alpha particles and there are no low-lying collective 0^+ states with which to test such calculations.

The single folding model was used by Bertrand *et al.* [4] to analyze 152 MeV inelastic alpha scattering to giant resonances, and they found that GMR cross sections obtained with the folding model were substantially below those obtained with the deformed potential model, which could account for the ''missing'' strength in ^{58}Ni [2]. However, both in the work of Bertrand *et al.* and the work of Morsch *et al.* [5], where the double folding model was used to analyze 172 MeV alpha scattering to giant resonances, the cross sections attributed to the GMR in ^{208}Pb considerably exceeded folding model predictions. Unfortunately, those data did not extend to the small angles necessary to identify the GMR and to separate it from other multipoles. Both authors speculate that the excess strength might be due to the presence of other multipolarities in the peaks. Youngblood *et al.* [6] used the deformed potential model for analysis of 129 MeV inelastic alpha scattering data taken at small angles where the monopole can be definitively identified, and generally for nuclei with $A>89$, 100% of the isoscalar $E0$ energy-weighted sum rule (EWSR) was located in a single broad peak near the giant quadrupole resonance. Satchler [7] compared results obtained with the deformed potential model and the single folding model for the ^{116}Sn data of Ref. [6]. The experimental cross section corresponded to about 180% of the $E0$ EWSR with the folding model and about 100% with the deformed potential model.

We have compared our $E_\alpha=129$ MeV data on both ^{58}Ni [8] and ^{208}Pb [6] to single folding model calculations, and the results are described here. We chose to compare to the 129-MeV data rather than our recent (much better) 240-MeV data because data from heavier targets are available and the alpha energy is not far from that of the extensive elastic scattering data at $E_\alpha=140$ MeV Bertrand *et al.* used to obtain folding model potentials and range. Also, Bertrand *et al.* did an extensive comparison to low-lying states as well as to their own elastic data to test the validity of their calculations. Our calculations used a Gaussian alpha-nucleon interaction with the range parameter $\alpha=1.94$ fm and potential depths obtained by Bertrand *et al.* [4] for ^{58}Ni and ^{208}Pb.

Since Bertrand *et al.* did not give the detailed parameters of the density distributions they used for ^{58}Ni or ^{208}Pb, we have used parameters from Satchler [9]. The parameters of the density distributions as well as the potential depths for the folding model calculations and the values of α_0^2 for 100% of the $E0$ EWSR [7] are shown in Table I. Folded potentials and form factors were obtained using the code DOLFIN [10] based on the work by Satchler and Love [11]. Optical model and DWBA calculations were carried out with the code PTOLEMY [12]. Cross sections for elastic scattering of 152-MeV alpha particles from ^{58}Ni and ^{208}Pb were calculated and

TABLE I. Parameters for folding model calculations.

Nucleus	c (fm)	a (fm)	$\langle r^2\rangle$ (fm^2)	α_0^2	E_x (MeV)	V (MeV)	W (MeV)
^{58}Ni	4.08	0.515	13.653	0.0194	17.0	35.5	21.5
^{208}Pb	6.67	0.545	30.798	0.00297	13.7	40.5	26.0

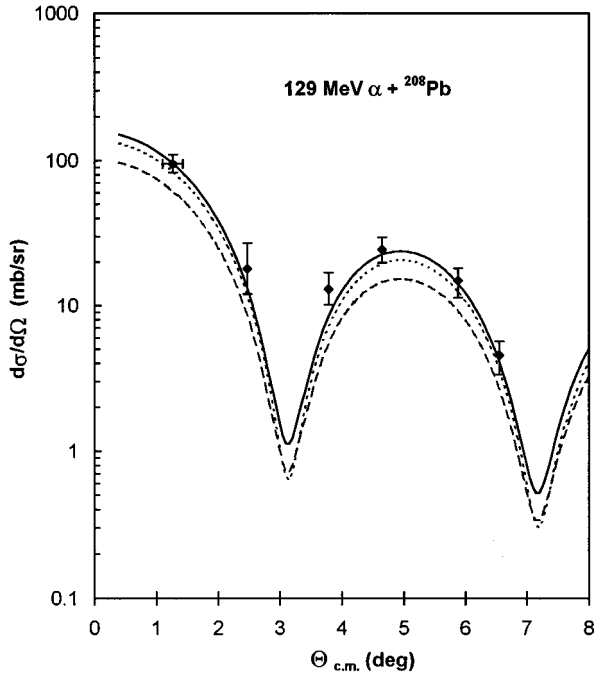

FIG. 1. Angular distribution of the differential cross section for the $E_x=13.7$ MeV peak in ^{208}Pb taken from Ref. [6]. The data have been plotted at their average angle (see text). DWBA calculations using both deformed potential and single folding models are shown for 100% of the $E0$ EWSR by lines with small and long dashes, respectively. The folding model calculation normalized to the data (160% $E0$ EWSR) is shown by the solid line.

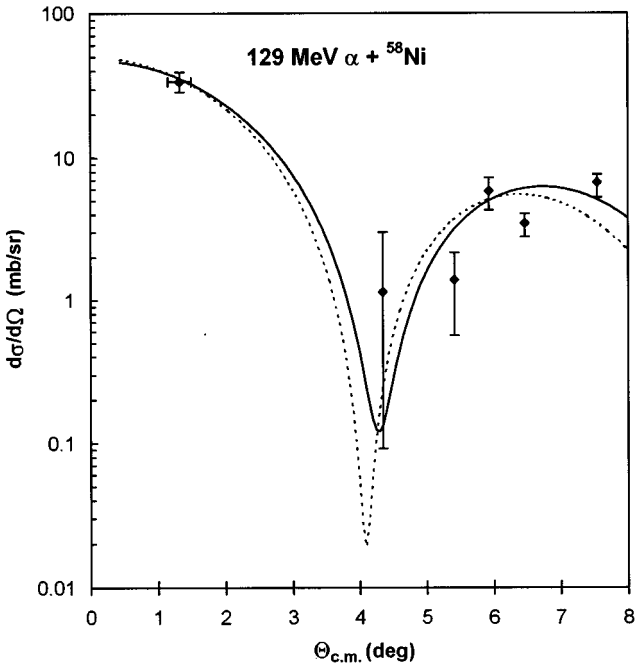

FIG. 2. Angular distribution of the differential cross section for the $E_x=17.0$ MeV peak in ^{58}Ni taken from Ref. [8]. The data have been plotted at their average angle (see text). DWBA calculations using both the deformed potential (23% $E0$ EWSR) and the folding model (40% $E0$ EWSR) are shown by the dashed and solid lines, respectively.

agreed with those shown by Bertrand *et al.* [4]. GMR cross sections calculated for ^{116}Sn agreed with those obtained by Satchler [7].

The transition density for the GMR is given by [7]

$$U=-\alpha_0[3\rho+r d\rho/dr],$$

where, for a state that exhausts the EWSR [7],

$$\alpha_0^2=2\pi(\hbar^2/m)(A\langle r^2\rangle E_x)^{-1}.$$

Generally, it has been customary to assume a uniform mass distribution and set $R^2=(5/3)\langle r^2\rangle$ and then use the potential radius for R. Since $R_p^2\approx 5/3\langle r^2\rangle_m$, this has the effect of setting the mass deformation parameter equal to the potential deformation parameter ($\alpha_m=\alpha_p$). The sum rule values obtained with the deformed potential model in this paper were obtained in this way. However, Satchler [7] has pointed out that to be consistent with what is done for other multipolarities, the deformation lengths should be equal ($\alpha_m c=\alpha_p R_p$), which has the effect of lowering the cross sections obtained with the deformed potential model.

The GMR cross sections for 129 MeV alpha scattering on ^{58}Ni and ^{208}Pb were calculated using the parameters shown in Table I. The results of these calculations are shown along with the data in Figs. 1 and 2. DWBA calculations were also carried out for both nuclei with the deformed potential model using parameters from Ref. [13] (Table II) and these are shown.

The data points shown in Refs. [6,8] at 0° were taken with a large solid angle and are shown here at the corresponding average angles. The θ error bars shown on this point represent an uncertainty in this average angle due to an uncertainty in the effective solid angle of the spectrometer at 0°. This does not affect the extracted cross section because calibrated known low-lying states in ^{12}C were used [6] to measure the solid-angle–dead-time product for all 0° runs. The other data points were taken with an opening of 0.6° (x) by 1.2° (y), and the DWBA calculations have been angle averaged over this opening. These 0° points are important because the dominant contribution to these is from the monopole resonance, and hence they are the best measure of the total monopole strength in the peak.

The sum rule percentages obtained with the different models are summarized in Table III. The experimental cross section for the peak at $E_x=17.0$ MeV in ^{58}Ni is fit well by a single folding model calculation corresponding to 40% of the $E0$ EWSR and by a deformed potential model calculation corresponding to 23% of the $E0$ EWSR. Adding 7% of the $E2$ EWSR, as required to fit the 240-MeV data [2], made the fits noticeably worse, but also made only a small change in the $E0$ strength. As the 240-MeV data is of much better quality, the disagreement in $E2$ strength is not significant. The cross section for the 13.7-MeV peak in ^{208}Pb corre-

TABLE II. Parameters for deformed potential calculations.

Nucleus	V (MeV)	W (MeV)	r_0 (fm)	a (fm)
^{58}Ni	78.9	38.0	1.28	0.90
^{208}Pb	89.3	52.7	1.35	0.71

TABLE III. $E0$ EWSR values from different analyses.

	^{58}Ni 17.0 MeV (%)	^{208}Pb 13.7 MeV (%)	Ratio Pb/Ni	Total[a] ^{58}Ni/^{208}Pb (%)
Deformed potential				
Uniform mass distribution	23	112	4.9	32±8
$\alpha_m c = \alpha_p R_p$	31	129	4.2	37±9
Single folding				
Gaussian −1.94	40	160	4.0	39±9
Density dependent[b]	42	154	3.6	42±10

[a]Total $E0$ strength in ^{58}Ni from Ref. [2] normalized assuming 100% $E0$ EWSR in Pb (see text).
[b]Ref. [16].

sponds to 160% of the $E0$ EWSR using the folding model and 112% using the deformed potential model (129% of the $E0$ EWSR with $\alpha_m c = \alpha_p R_p$). As Bertrand *et al.* speculated that significant components of higher multipolarities might be present in their data and might account for the large EWSR values they obtain with the folding model, we also show a calculation with 25% of the $E4$ EWSR present in Fig. 3. This has little effect on the $E0$ EWSR (because of the small angle data point) and makes the fit poorer to the larger angle data points. Other multipolarities will result in similar poor fits to the larger angle data points before making substantial contributions to the small angle cross section. Thus contributions from higher multipolarities can be ruled out as the source of excessive $E0$ sum rule strengths obtained for the GMR in ^{208}Pb.

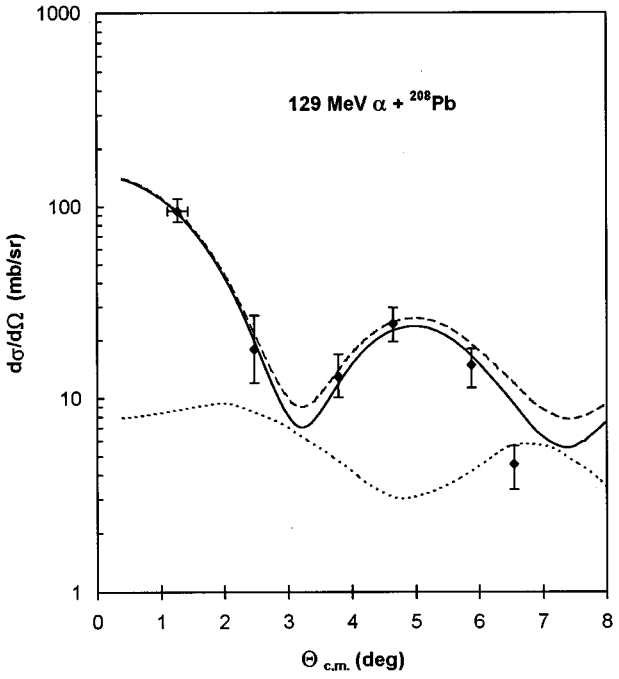

FIG. 3. Angular distribution of the differential cross section for the $E_x = 13.7$ MeV peak in ^{208}Pb taken from Ref. [6]. The data have been plotted at their average angle (see text). DWBA calculations using the deformed potential model are shown by the lines. The solid line is for 100% of the $E0$ EWSR plus 100% of the $E1$ EWSR. The short dashes are for 100% of the $E1$ EWSR (from Ref. [14]). The long dashes are for 100% of the $E0$ EWSR plus 100% $E1$ EWSR plus 25% $E4$ EWSR.

In ^{208}Pb the giant dipole resonance (GDR) is unresolved from the GMR, but Satchler [7], Shlomo *et al.* [14], and Poelhekken *et al.* [15] have shown that the GDR cross section is small compared to the GMR for 129 MeV alpha scattering. For completeness, we show a fit to the ^{208}Pb data for 100% of strengths of the GDR and GMR obtained using the deformed potential model in Fig. 3. This fits the data reasonably well.

The sum rule fractions reported here for the deformed potential model are somewhat different from those reported in Refs. [6,8] because in this work more emphasis was placed on the 0° data point, which is the best measure of monopole strength.

Also included in the last row in Table III are results from Satchler [16] for a single folding calculation using a density-dependent interaction. These were obtained by fitting 140-MeV elastic scattering data, but using a hybrid potential where the real part is obtained from folding while the imaginary part is a Woods-Saxon potential. This was necessary to fit the elastic scattering data over the entire angle range available. The model is described in Ref. [17]. The results are close to those obtained with the Gaussian interaction, though the ratio of Ni to Pb strength is about 10% higher.

In Ref. [2] the $E_x = 17$ MeV resonance in ^{58}Ni was found to contain 22% of the $E0$ EWSR with an additional 10% in a peak at $E_x = 20.8$ MeV. These strengths were obtained with the deformed potential model assuming a uniform mass distribution. As is apparent from Table III, for the $E_\alpha = 129$ MeV data the extracted $E0$ sum rule strength is dependent on model assumptions, even though the breathing mode transition density was used for all calculations. In fact, the $E0$ strength extracted from either of the folding calculations is considerably higher for both Ni and Pb and, in Pb, considerably exceeds the sum rule. Thus the best measure of the $E0$ strength in Ni may be the ratio of total $E0$ strength found in ^{58}Ni to that in the $E_x = 13.7$ MeV state in ^{208}Pb, and this is given in the last column of Table III. For this we have assumed that the ratio of Ni to Pb sum rule strengths obtained for each model with $E_\alpha = 129$ MeV are appropriate for $E_\alpha = 240$ MeV. As the GDR contributions in ^{208}Pb are small and approximately the same for each calculation, they have been ignored. The GDR contribution was explicitly accounted for in the 240-MeV analysis [2] of Ni. With these assumptions, the two folding models give (39±9)% and (42 ±10)% for the total $E0$ strength located in ^{58}Ni (at $E_\alpha = 240$ MeV). The uncertainties listed include those of the 240-MeV

measurement and those due to the uncertainty in the cross sections for the 0° data, all summed in quadrature. The uncertainty in average angle does not affect this ratio as the average angle was the same for the Ni and Pb data. The experimental uncertainties on the individual sum rule values are about $\pm 20\%$.

The excessive strength obtained for ^{208}Pb using the folding model is consistent with the result of Satchler [7] for alpha scattering data from ^{116}Sn. Horen *et al.* [18] reported a similar problem in heavy-ion scattering. Cross sections obtained with the folding model are about a factor of 2 less than those obtained experimentally in heavy-ion scattering for the GMR. However, one must contend with two experimental problems when extracting GMR strength from heavy-ion scattering. The GMR is unresolved from the giant dipole resonance, which is strongly excited by heavy ions, and so the GMR cross section can be obtained only after subtracting a relatively strong GDR. Also, the angular distributions obtained in heavy-ion scattering are not characteristic of L, and so there is not a clear signature that the peak being analyzed is 0^+.

The underprediction of the $E0$ cross section for heavier nuclei must be understood if the folding model is to be used to extract strengths of the GMR in nuclei. I point out that a breathing mode transition density was used for all of these calculations, which is a source of uncertainty. Chomaz *et al.* [19] performed calculations for 152 MeV alpha scattering with microscopic and collective breathing mode form factors and found that the breathing mode form factors underpredicted the cross sections for ^{208}Pb and ^{60}Ni by 20% and 10%, respectively.

I thank Shalom Shlomo and Ray Satchler for very helpful discussions regarding both monopole sum rules and folding model calculations and Ray Satchler for providing the density-dependent folding calculations. This work was supported in part by the Department of Energy under Grant No. DE-FG03-93ER40773 and by The Robert A. Welch Foundation.

[1] S. Shlomo and D. H. Youngblood, Phys. Rev. C **47**, 529 (1993).
[2] D. H. Youngblood, H. L. Clark, and Y.-W. Lui, Phys. Rev. Lett. **76**, 1429 (1996).
[3] J. R. Beene, D. J. Horen, and G. R. Satchler, Nucl. Phys. **A596**, 137 (1996); Phys. Lett. B **344**, 67 (1995); Phys. Rev. C **48**, 3128 (1993).
[4] F. E. Bertrand, G. R. Satchler, D. J. Horen, J. R. Wu, A. D. Bacher, G. T. Emery, W. P. Jones, D. W. Miller, and A. van der Woude, Phys. Rev. C **22**, 1831 (1980).
[5] H. P. Morsch, C. Sukosd, M. Rogge, P. Turek, H. Machner, and C. Mayer-Boricke, Phys. Rev. C **22**, 489 (1980).
[6] D. H. Youngblood, P. Bogucki, J. D. Bronson, U. Garg, Y.-W. Lui, and C. M. Rozsa, Phys. Rev. C **23**, 1997 (1981).
[7] G. R. Satchler, Nucl. Phys. **A472**, 215 (1987).
[8] D. H. Youngblood and Y.-W. Lui, Phys. Rev. C **44**, 1878 (1991).
[9] G. R. Satchler, Nucl. Phys. **A579**, 241 (1994).
[10] L. D. Rickertsen, Computer code DOLFIN, 1976 (unpublished).
[11] G. R. Satchler and W. G. Love, Phys. Rep. **55**, 183 (1979).
[12] M. Rhoades-Brown, M. H. Macfarlane, and S. C. Pieper, Phys. Rev. C **21**, 2417 (1980); M. H. Macfarlane and S. C. Pieper, Argonne National Laboratory Report No. ANL-76-11, Rev. 1, 1978 (unpublished).
[13] D. H. Youngblood, J. M. Moss, C. M. Rozsa, J. D. Bronson, A. D. Bacher, and D. R. Brown, Phys. Rev. C **13**, 994 (1976).
[14] S. Shlomo, Y.-W. Lui, D. H. Youngblood, T. Udagawa, and T. Tamura, Phys. Rev. C **36**, 1317 (1987).
[15] T. D. Poelhekken, S. K. B. Hesmondhalgh, H. J. Hofmann, H. W. Wilschut, A. van der Woude, and M. N. Harakeh, Phys. Rev. Lett. **62**, 16 (1989).
[16] G. R. Satchler (private communication).
[17] G. R. Satchler and Dao T. Khoa, Phys. Rev. C (to be published).
[18] D. J. Horen, J. R. Beene, and G. R. Satchler, Phys. Rev. C **52**, 1554 (1995).
[19] Ph. Chomaz, Tiina Suomijarvi, N. Van Giai, and J. Treiner, Phys. Lett. B **281**, 6 (1992).